Title
A 48-to-6 V Multi-Resonant-Doubler Switched-Capacitor Converter for Data Center Applications

ISBN
9781728148298

Authors
Ye, Zichao
Abramson, Rose A
Pilawa-Podgurski, Robert CN

Publication Date
2020-03-19

DOI
10.1109/apec39645.2020.9124384

2020 IEEE Applied Power Electronics Conference and Exposition
New Orleans, LA, USA

A 48-to-6 V Multi-Resonant-Doubler Switched-Capacitor Converter for Data Center Applications

Z. Ye
R. A. Abramson
R. C. N. Pilawa-Podgurski

A 48-to-6 V Multi-Resonant-Doubler Switched-Capacitor Converter for Data Center Applications

Zichao Ye, Rose A. Abramson and Robert C.N. Pilawa-Podgurski
Department of Electrical Engineering and Computer Sciences
University of California, Berkeley
Email: {yezichao, rose_abramson, pilawa}@berkeley.edu

***Abstract*—Compared with conventional switched-capacitor (SC) converters with two operating phases, multi-phase SC converters can achieve the same conversion ratio with fewer capacitors and switches. This feature makes multi-phase SC converters an attractive candidate for applications with large conversion ratios. To further improve the performance by enabling soft-charging and soft-switching operations, SC converters can be transformed to resonant switched-capacitor (ReSC) converters with augmented inductor(s). This work presents an 8-to-1 multi-phase ReSC converter design that features the least-possible number of switches and capacitors for the achieved gain. Both theoretical analysis and experimental results from a practical implementation are provided to demonstrate the benefits of the multi-phase resonant approach. A 48-to-6 V converter prototype with 40 A output current for data center applications was built and tested. The prototype achieved 98.6% peak efficiency (98.0% including gate drive loss) and 1675 W/in^3 power density, achieving one of the best overall in-class performances.**

I. Introduction

The power consumption of data centers is continuously growing, leading to efforts to distribute the power at higher server input voltages (e.g., 48 V) to reduce the cabling and busbar conduction losses. A major challenge in such systems is the conversion from the 48 V bus to the extreme low voltage and high current operating levels of CPUs and GPUs. To address such a high step-down conversion ratio, a two-stage approach is usually required. One typical solution is a 48-to-12 V bus converter followed by a 12-to-1 V point-of-load (POL) converter. However, recent research [1] suggests that a lower intermediate bus voltage (e.g. 6 V) may provide higher overall efficiency, once both the intermediate bus converter and the second-stage buck converter are considered. Therefore, there is increased interest in highly efficient 48-to-6 V conversion. Recently, a GaN-based 48-to-6 V fixed ratio LLC converter has been demonstrated with 98% peak efficiency and 1100 W/in^3 power density [2], which used an 8:1 matrix transformer to step down the voltage.

Besides transformer-based solutions, a number of high performance resonant switched-capacitor (ReSC) works have also achieved excellent performance [3]–[5]. In addition to the traditional benefits of SC converters (i.e., efficient utilization of switches, higher energy density of capacitors [6]), the resonant inductor in ReSC converters allows for soft-charging and soft-switching operations [7], [8] that can further improve the efficiency and power density. However, the majority of existing works focus on 4-to-1 or 6-to-1 ratios, and high performance ReSC works with higher conversion ratios have not been widely demonstrated. This is because the number of components (switches and capacitors) increases proportionally with respect to the conversion ratio, and the increased circuit implementation complexity can potentially reduce the theoretical performance benefits.

Compared with typical SC converters (such as the Dickson and series-parallel) which have two operating phases, multi-phase SC converters can achieve the same conversion ratio with significantly fewer switches and flying capacitors [9]. Even though multi-phase SC converters have been explored previously [10], prior focus has been on variable conversion ratios [11], [12] for voltage regulation purposes. This work builds upon multi-phase SC converters by implementing them for high conversion ratio applications. An 8-to-1 multi-phase voltage doubler operating in resonant mode (named Multi-Resonant-Doubler) that features the least-possible number of switches and capacitors is proposed and analyzed in detail. It will be shown that even though the multi-resonant-doubler does not have a significant advantage in switch utilization compared to other two-phase SC converters, it has superior passive component utilization, as well as additional benefits in practical implementations. A 48-to-6 V, 40 A, fixed ratio converter prototype was designed and implemented. The prototype achieved 98.6% peak efficiency (98.0% including gate drive loss) and 1675 W/in^3 power density, achieving one of the best overall in-class performances.

II. Multi-Resonant-Doubler Converter

A. Theoretical performance limit of SC converters

According to [9], [13], for two-phase SC converters, the realizable conversion ratio with k capacitors ($k-1$ flying capacitors and one output capacitor) is bounded by the kth Fibonacci number F_k:

$$M[k] = \frac{V_{\text{out}}}{V_{\text{in}}} = \frac{1 \leq P[k] \leq F_k}{1 \leq Q[k] \leq F_k} \tag{1}$$

where $F_1 = 1, F_2 = 2, F_3 = 3, ..., F_n = F_{n-1} + F_{n-2}$. Similarly, the bound on the number of switches required in any SC circuit is found to be $3k-2$. Intuitively, the voltage gain is achieved by capacitor voltage addition (or subtraction) in two-phase SC converters. By adding (or subtracting) the voltage of every two neighboring flying capacitors by turns, the capacitor voltages and the output voltage increases (or decreases) in a

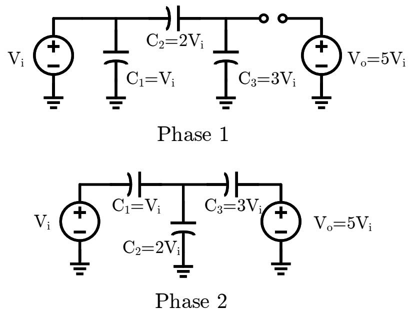

Fig. 1: The maximum voltage gain in two-phase SC converter follows the Fibonacci sequence.

Fibonacci fashion, achieving the maximum achievable voltage gain. The two operating phases of a Fibonacci step-up converter with three flying capacitors C_1, C_2, C_3 are shown in Fig. 1. In phase 1, C_1 is charged to the input voltage V_{i} and C_3 is charged by the series combination of C_1 and C_2 to $3V_{\mathrm{i}}$. In phase 2, C_2 is charged by the series combination of C_1 and input voltage to $2V_{\mathrm{i}}$, whereas the output voltage is charged by C_2 and C_3 to $5V_{\mathrm{i}}$. A property of the Fibonacci sequence is that the ratio of every two successive Fibonacci numbers approaches the golden ratio (1.618). It indicates that the fastest possible voltage growth rate (with respect to the number of flying capacitor) of a two-phase SC converter is 1.618.

As discussed in [14], given the same number of capacitors and switches, if multiple operating phases can be introduced, the maximum realizable gain with k capacitors becomes

$$M[k]_{max} = 2^{k-1} \tag{2}$$

which is greater than the Fibonacci bound. From a circuit perspective, this can be implemented by a chain of 2-to-1 voltage doublers, which effectively achieves capacitor voltage multiplication (or division). As shown in Fig. 2, a voltage doubler with three flying capacitors C_1, C_2, C_3 can achieve a gain of 8. However, with two-phase operation, the voltage doubler requires two intermediate decoupling capacitors C_{out1} and C_{out2}, resulting in a total required capacitor number that is higher than that predicted in (2). One method to eliminate the intermediate decoupling capacitors is to operate two two-phase doublers in parallel with interleaving control [3]. Alternatively, more operating phases can be added such that some flying capacitors are disconnected from the circuit for some phases, thereby relaxing the intermediate decoupling requirement [15]. The multi-phase voltage doubler in Fig. 2 can achieve the maximum theoretical gain of (2) with 4 capacitors (3 flying capacitors and one output capacitor). Note that even though the gain becomes 2^{k-1} for multi-phase operation, the minimum number of switches required remains $3k-2$. It indicates that it is possible to further reduce the switch number of the multi-phase voltage doubler in Fig. 2, from 12 switches to the theoretical minimum of 10 switches while keeping the voltage gain at 8.

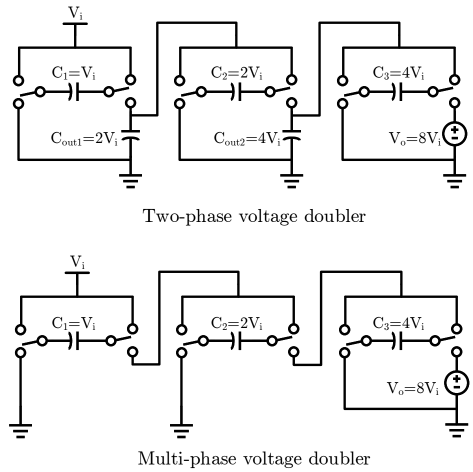

Fig. 2: Exponential growth of voltage gain with voltage doublers.

B. Proposed topology and operating principle

The schematic drawing of the proposed four-phase 8-to-1 ReSC converter is shown in Fig. 3. Its fundamental multi-phase structure was first proposed in [10]. It can be viewed as one practical circuit implementation of a multi-phase voltage doubler that achieves the theoretical maximum gain with the least number of components (3 flying capacitors and 10 switches for a gain of 8). This work proposes a new implementation of this structure, herein named the Multi-Resonant-Doubler, by adding a resonant inductor at the switch node and then operating the circuit as a multi-phase resonant switched-capacitor converter.

Because of the voltage doubler structure, the flying capacitors carry binary voltages ($C_1 = 4V_o$, $C_2 = 2V_o$, $C_3 = V_o$) and the switches see the same voltage as that of the corresponding capacitors ($Q_{1-4} = 4V_o$, $Q_{5-7} = 2V_o$, $Q_{8-10} = V_o$). The key control signals, inductor and capacitor current waveforms, and the equivalent circuit of the four operating phases are shown in Fig. 4. It can be seen that all flying capacitors are charged and discharged in a resonant fashion, resulting in soft-charging and zero-current switching (ZCS). The detailed operation of the four phases are as follows:

- Phase 1: The "Ph1", "Ph12" and "Ph123" switches in Fig. 3 are ON. C_1, C_2, C_3 and L are connected in series. All flying capacitors are resonantly charged by the input. The duration of phase 1 is $\frac{1}{8}$ of the switching cycle. The equivalent resonant frequency of this phase is $f_{r,\mathrm{ph1}} = \frac{1}{2\pi\sqrt{LC_{eq1}}}$, where $\frac{1}{C_{eq1}} = \frac{1}{C_1} + \frac{1}{C_2} + \frac{1}{C_3}$.
- Phase 2: The "Ph2", "Ph12" and "Ph123" switches are ON. In this phase, all flying capacitors are still connected in series, but C_1 is being discharged. The length of the phase and the equivalent resonant frequency remain the same as those of phase 1.
- Phase 3: The "Ph3" and "Ph123" switches are ON. In this phase, C_1 is disconnected and C_3 is only charged

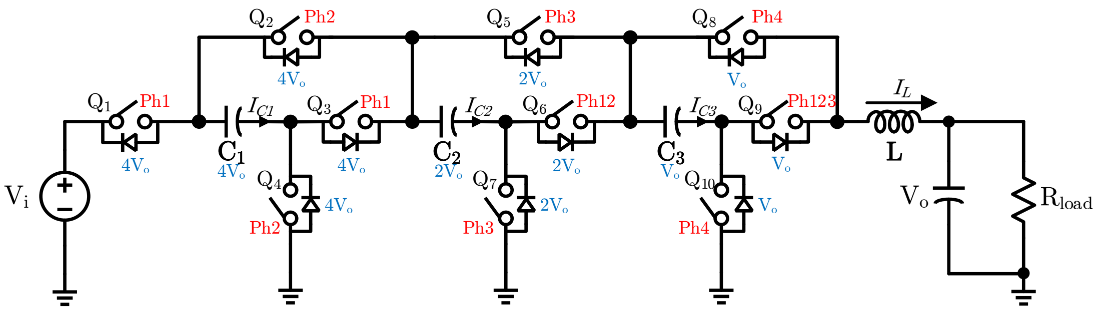

Fig. 3: Schematic drawing of the proposed multi-resonant-doubler converter with device ratings and control signals labeled.

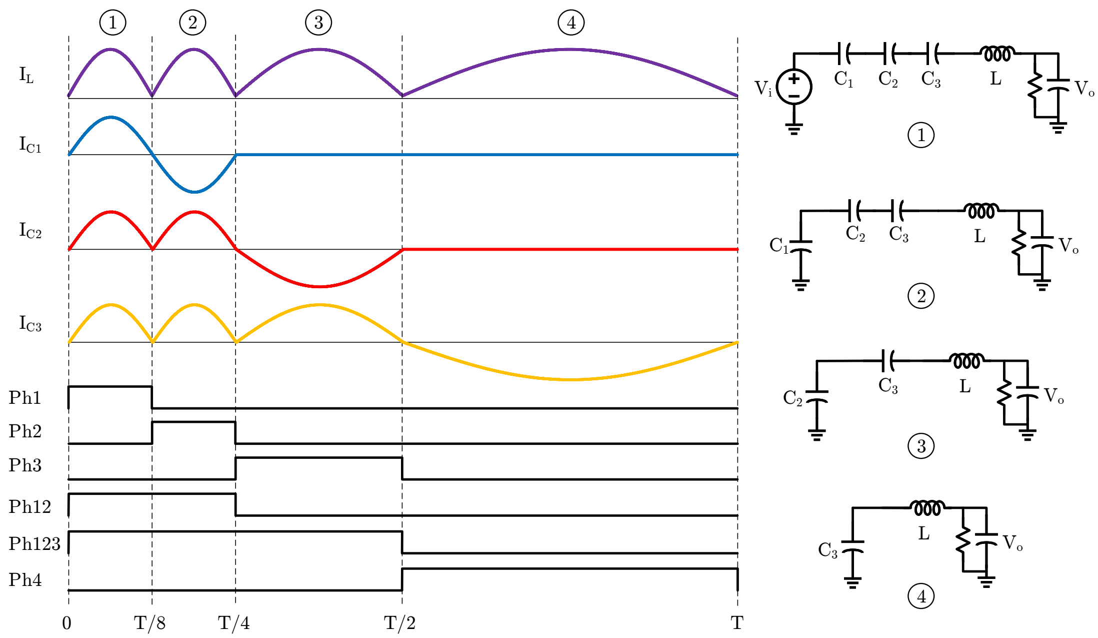

Fig. 4: Inductor and capacitor current waveforms and control signals of the multi-resonant-doubler converter.

by C_2. In order to maintain capacitor charge balance, the duration of this phase is doubled to $\frac{1}{4}$ of the switching cycle. The equivalent resonant frequency of this phase is now $f_{r,\text{ph3}} = \frac{1}{2\pi\sqrt{LC_{eq3}}}$, where $\frac{1}{C_{eq3}} = \frac{1}{C_2} + \frac{1}{C_3}$.

- Phase 4: Only the "Ph4" switches are ON. In this phase, both C_1 and C_2 are disconnected and C_3 is resonantly discharged to the load. The equivalent resonant frequency of this phase is $f_{r,\text{ph4}} = \frac{1}{2\pi\sqrt{LC_3}}$. Since the duration of this phase is $\frac{1}{2}$ of the switching cycle, the overall switching frequency with four phases combined would be the same as $f_{r,\text{ph4}}$ ($f_{\text{sw}} = f_{r,\text{ph4}} = \frac{1}{2\pi\sqrt{LC_3}}$), which is only determined by L and C_3.

By equating the relative length of different phases and the corresponding resonant frequency, the required ratio of the flying capacitors can be found to be $C_1 = \frac{1}{12}C_3$ and $C_2 = \frac{1}{3}C_3$. These reduced capacitance requirements are due to the fact that the resonant charging currents of C_1 and C_2 are at higher frequencies than C_3. It indicates that even though C_1 and C_2 must be rated for higher voltages than C_3, their physical volume could still be very similar due to their reduced capacitance. Moreover, these capacitor ratios relate to two operation constraints. First, these exact ratios are needed to achieve ZCS for all switches. Second, these ratios determine the minimal capacitor values that are needed to achieve soft-charging operation. In practical implementations, it is very challenging to maintain an exact capacitor ratio. Nevertheless, the soft-charging operation is guaranteed as long as the actual capacitors exceed their minimum required values. In practice, the imperfect ZCS operation due to capacitor ratio mismatch was found to have a relatively minor effect on the performance of the converter.

C. *Comparison with two-phase SC converters*

For discrete low-voltage applications, both the number of switches (and the associated gate drive circuitry) and the number of passive components can greatly affect the solution size. As shown in Table I, the multi-resonant-doubler uses the least number of switches, capacitors, and inductors. Moreover, when considering the total passive component volume from the fundamental energy transfer perspective, it is found that doubler-based topologies have superior passive component

TABLE I: Comparison of number of components for 8-to-1 resonant switched-capacitor converters

Topology	Switch number	Flying capacitor number	Inductor number	R_{out} (assuming same R for all switches)
Multi-Resonant-Doubler	10 ($4V_o\times4$, $2V_o\times3$, $V_o\times3$)	3 ($4V_o$, $2V_o$, V_o)	1	2.75 (10 switches), 2 (13 switches), 1.25 (22 switches)
Cascaded Resonant [3]	12 ($4V_o\times4$, $2V_o\times4$, $V_o\times4$)	3 ($4V_o$, $2V_o$, V_o)	3	2.625 (12 switches), 1.625 (16 switches), 1.125 (24 switches)
Fibonacci	13 ($5V_o\times2$, $3V_o\times4$, $2V_o\times3$, $2V_o\times4$)	4 ($5V_o$, $3V_o$, $2V_o$, V_o)	1	2.165 (13 switches), 1.4775 (16 switches)
Series-Parallel	22 ($7V_o\times3$, $6V_o$-$2V_o\times2$, $V_o\times9$)	7 ($V_o\times7$)	1	1.25 (22 switches)
Switched Tank (Dickson) [4]	22 ($2V_o\times6$, $V_o\times16$)	7 ($7V_o$, $6V_o$, ... , V_o)	4	0.8 (22 switches)

utilization among all hybrid SC topologies [16]. Because of these reasons, the multi-resonant-doubler has the potential to achieve higher power density than its two-phase counterparts.

Nevertheless, the switch number reduction is not free and will result in higher output impedance (which negatively impacts efficiency). As shown in Table I, assuming all switches have the same on-resistance R for low-voltage applications, the output impedance of the multi-resonant-doubler is 2.75R with the minimum number of switches (10 switches), which is higher than the other topologies. If conduction loss is a major concern, more switches can be paralleled in the key current path, resulting in comparable output impedance to other topologies with a similar number of total switches. Fundamentally, there is no win-win situation that can achieve low component count and low output impedance simultaneously. The Dickson and series-parallel converters can have low output impedance because they use a large number of switches to split the current into multiple parallel paths. In comparison, the multi-resonant-doubler uses less switches but has only one current path and thereby higher output impedance.

However, in practical implementations, the multi-resonant-doubler's low required switch count can make it more adaptable to different applications compared to two-phase topologies with an inherently large number of switches and gate drivers. Depending on the design specifications, more switches can be paralleled to reduce the output impedance, without requiring additional gate drive circuits. In addition, the low component count can greatly simplify the PCB layout and increase power density. Since PCB loss contributes a large portion to the overall loss for low-voltage high-current applications, a clean and simple PCB layout is important for a high performance design.

III. Hardware Implementation and Experimental Results

An annotated photograph of the hardware prototype is shown in Fig. 5, with key components highlighted. Table II provides the main operating parameters of the converter and Table III lists the specifications of the main components. Thanks to the reduced-voltage stress of the doubler topology, low voltage silicon MOSFETs can be used (40 V for Q_{1-4} and 25 V for Q_{5-10}). In order to reduce the output impedance, Q_{8-10} are each implemented with two paralleled switches, one on each side of the board. The cascaded bootstrap method [17] is used to power the floating gate drivers. The PCB has 4 layers and is fabricated with 4 oz copper on the outer layers (where the critical conduction path is) and 3 oz copper on the inner layers.

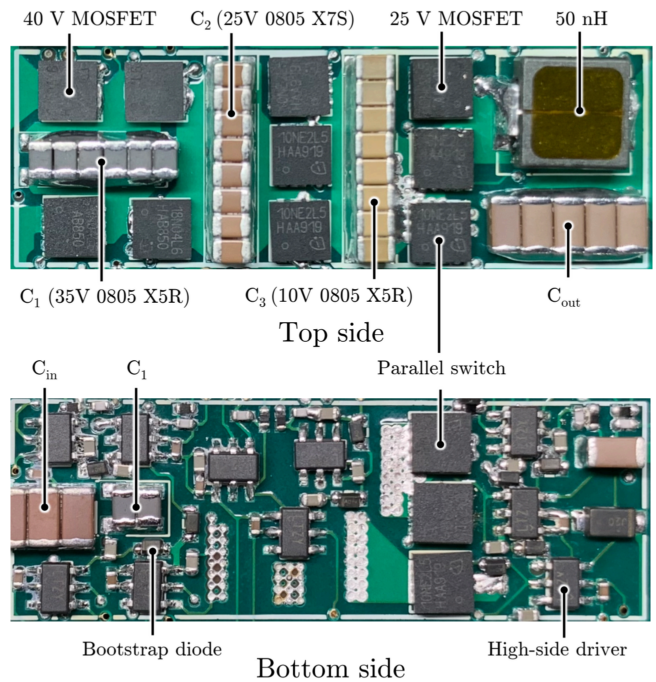

Fig. 5: Photograph of the converter prototype. Dimensions: 1.38 × 0.46 × 0.22 inch (3.5 × 1.17 × 0.55 cm).

TABLE II: Key Converter Parameters

	Nominal	Range
Input voltage	48 V	40 – 60 V
Output voltage	6 V	5 – 7.5 V
Output current	40 A	40 A
Power rating	240 W	200 – 300 W
Switching frequency	70 kHz	70 – 78 kHz

The minimum switching frequency is determined by the inductor and the capacitor C_3, where $f_{\mathrm{sw,min}} = \frac{1}{2\pi\sqrt{LC_3}}$. However, as discussed in [3], to counteract the effects of component non-idealities and further reduce the conduction loss, the converter can operate at a frequency that is slightly higher than resonance, at the expense of imperfect ZCS operation and slightly increased switching loss. For this prototype, $f_{\mathrm{sw,min}} = 52$ kHz and the actual switching frequency is 70 kHz when operating at 48-to-6 V. Measured waveforms of inductor current and switch node voltage are shown in Fig. 6. The converter is also able to handle large load transients. In Fig. 7, the output voltage does not show significant undershoot

TABLE III: Main Component Listing of the Multi-Resonant-Doubler Converter

Component	Part number	Parameters
Switch Q_1-Q_4	Infineon BSZ018N04LS6	40 V, 1.8 mΩ
Switch Q_5-Q_{10}	Infineon BSZ010NE2LS5	25 V, 1 mΩ
Flying capacitor C_1	TDK C2012X5R1V226M125AC	X5R, 35 V, 22 μF*$\times$14
Flying capacitor C_2	TDK C2012X7S1E106K125AC	X7S, 25 V, 10 μF*$\times$16
Flying capacitor C_3	Murata GRM21BR61A476ME15L	X5R, 10 V, 47 μF*$\times$16
Resonant inductor L	Coilcraft SLC7530S-500ML	50 nH, 50 A I_{sat}
Gate driver	Analog Devices LTC4440	80 V, high-side
Bootstrap diode	Infineon BAT6402VH6327XTSA1	40 V, Schottky

* The capacitance listed here is the nominal value before dc derating.

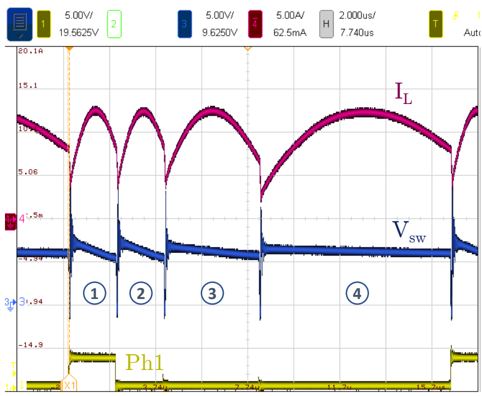

Fig. 6: Waveform of inductor current and switch node voltage.

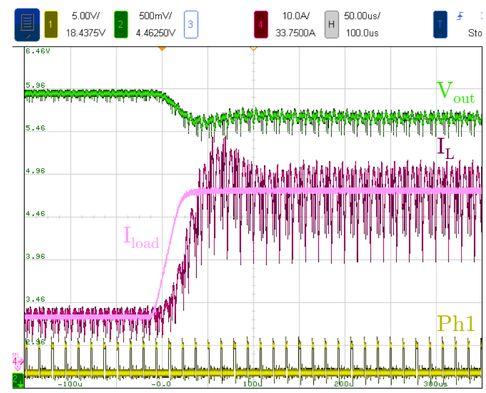

Fig. 7: Load-step from 10 A to 40 A for 48 to 6 V.

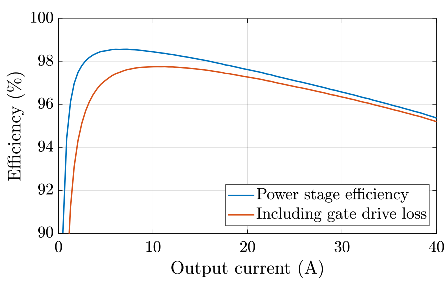

(a) 40 to 5 V (f_{sw} = 70 kHz).

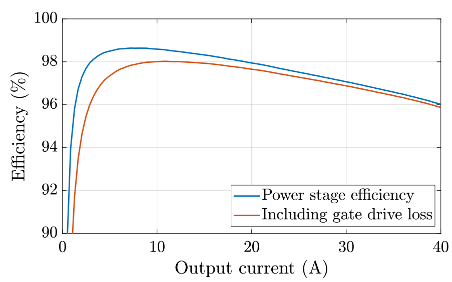

(b) 48 to 6 V (f_{sw} = 70 kHz).

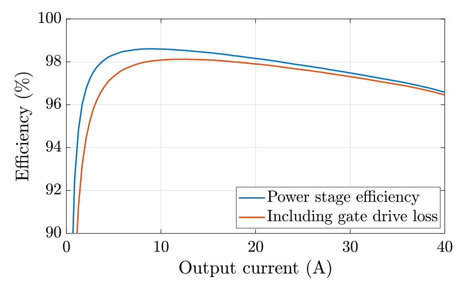

(c) 60 to 7.5 V (f_{sw} = 78 kHz).

Fig. 8: Measured efficiency at various input voltages.

after a 10 A to 40 A load step and stabilizes within a few switching cycles.

The converter has been tested up to 40 A output current. Based on the volume of the smallest rectangular box that can contain the converter, the power density is 1675 W/in^3 (102 kW/L) for 48-to-6 V conversion and 2100 W/in^3 (128 kW/L) for 60-to-7.5 V conversion. The efficiency was measured with a Yokogawa WT3000E precision power meter, and the results are plotted in Fig. 8 for various input voltages. For the nominal 48-to-6 V conversion, the peak efficiency is 98.6% (98.0% including gate drive loss). The full load efficiency at 40 A is 96.0% (95.9% including gate drive loss). The high efficiency performance can greatly reduce the thermal management requirement. As shown in Fig. 9, the converter maintains a maximum temperature of around 60°C at full power with fan cooling only. Additionally, the high efficiency also reduces the impact of load regulation. Even though the converter operates in fixed ratio mode (open loop), the output voltage only droops 250 mV (4.2% of V_{out}) at full load as depicted in Fig. 10.

Table II compares this work with some of the best existing works. Compared with the best in-class LLC converter [2], this work has very similar efficiency performance, but can achieve 50% more power density with much lower power rating. This makes it easy to be placed very close to the actual load to minimize the power distribution loss, while maintaining the flexibility to scale up for higher power needs. Since there are no other 8-to-1 SC works for this application

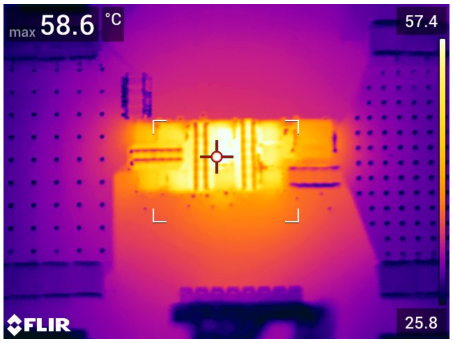

Fig. 9: Thermal performance with fan cooling only (V_{in} = 48 V, I_{out} = 40 A).

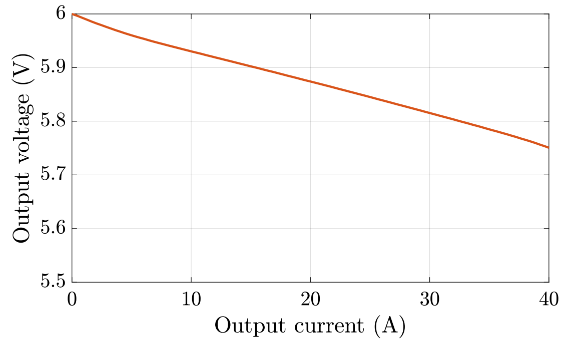

Fig. 10: Load regulation (V_{in} = 48 V, V_{out} = 6 V).

TABLE IV: Comparison of this work and existing high step-down ratio bus converters

Reference	Topology	Voltage ratio	Output current	Power Density (W/inch^3)	System Efficiency	Notes
this work	Resonant Multi-phase Doubler	48-to-6 V	40 A	1675	full load: 95.9% peak: 98.0%	fixed-ratio, silicon MOSFET
EPC AppNote014 [2]	LLC	48-to-6 V	150 A	1100	full load: 96.9% peak: 98.0%	fixed-ratio, Gen-5 GaN FET
EPC9205 [18]	Buck	48-to-6 V	14 A	$\leq$ 900	full load: 91.8% peak: 93.9%	Gen-5 GaN FET
Google Switched-Tank [4]	Resonant Dickson	54-to-13.5 V	50 A	500	full load: 97.41% peak: 98.61%	54 V input, 4:1 fixed-ratio, components are not densely populated

yet, we also compare the results with the 4-to-1 switched-tank converter [4]. Although the efficiency is slightly lower, the multi-resonant-doubler can achieve doubled conversion ratio with much higher power density.

IV. Conclusions

In this work, a resonant multi-phase doubler switched-capacitor converter is proposed to address the large step-down required from the 48 V bus in modern data center power delivery architectures. Compared with two-phase operation, the multi-phase operation can achieve the same conversion ratio with significantly fewer capacitors and switches, leading to potentially better power density and efficiency performance. A 48-to-6 V, 40 A converter prototype is built and tested, with 98.6% peak efficiency (98.0% including gate drive loss) and 1675 W/in^3 power density. These results show great promise for implementing a 6 V intermediate bus voltage.

References

[1] A. Lidow, "Powering graphics processors from a 48-v bus," 2019. [Online]. Available: https://www.powerelectronictips.com/powering-graphics-processors-from-a-48-v-bus/

[2] EPC Inc., *How to Exceed 98% Efficiency in a Compact 48 V to 6 V, 900 W LLC Resonant Converter Using eGaN FETs*, 2018. [Online]. Available: https://epc-co.com/epc/Portals/0/epc/documents/application-notes/How2AppNote014\%20Exceed\%2098\%20percent\%20Efficiency\%2048\%20V\%20to\%206\%20V\%20Resonant\%20Converter.pdf

[3] Z. Ye, Y. Lei, and R. C. N. Pilawa-Podgurski, "The cascaded resonant converter: A hybrid switched-capacitor topology with high power density and efficiency," *IEEE Transactions on Power Electronics*, pp. 1–1, 2019.

[4] S. Jiang, S. Saggini, C. Nan, X. Li, C. Chung, and M. Yazdani, "Switched tank converters," *IEEE Transactions on Power Electronics*, vol. 34, no. 6, pp. 5048–5062, June 2019.

[5] W. C. Liu, Z. Ye, and R. C. N. Pilawa-Podgurski, "A 97% peak efficiency and 308 A/in^3 current density 48-to-4 v two-stage resonant switched-capacitor converter for data center applications," in *2020 IEEE Applied Power Electronics Conference and Exposition (APEC)*, March 2020.

[6] M. D. Seeman and S. R. Sanders, "Analysis and optimization of switched-capacitor dc-dc converters," *IEEE Transactions on Power Electronics*, vol. 23, no. 2, pp. 841–851, March 2008.

[7] R. C. N. Pilawa-Podgurski, D. M. Giuliano, and D. J. Perreault, "Merged two-stage power converter architecture with soft charging switched-capacitor energy transfer," in *2008 IEEE Power Electronics Specialists Conference*, June 2008, pp. 4008–4015.

[8] Y. Lei and R. C. N. Pilawa-Podgurski, "A general method for analyzing resonant and soft-charging operation of switched-capacitor converters," *IEEE Transactions on Power Electronics*, vol. 30, no. 10, pp. 5650–5664, Oct 2015.

[9] M. S. Makowski, "Realizability conditions and bounds on synthesis of switched-capacitor dc-dc voltage multiplier circuits," *IEEE Transactions on Circuits and Systems I: Fundamental Theory and Applications*, vol. 44, no. 8, pp. 684–691, Aug 1997.

[10] I. Oota, F. Ueno, and T.Inoue, "Analysis of a switched-capacitor transformer with a large voltage-transformer-ratio and its applications," *Electronics and Comm. in Japan, Part 2*, vol. 73, no. 1, pp. 85–96, 1990.

[11] S. Ben-Yaakov and A. Kushnerov, "Algebraic foundation of self adjusting switched capacitors converters," in *2009 IEEE Energy Conversion Congress and Exposition*, Sep. 2009, pp. 1582–1589.

[12] S. Ben-Yaakov and M. Evzelman, "Generic and unified model of switched capacitor converters," in *2009 IEEE Energy Conversion Congress and Exposition*, Sep. 2009, pp. 3501–3508.

[13] M. S. Makowski and D. Maksimovic, "Performance limits of switched-capacitor dc-dc converters," in *Proceedings of PESC '95 - Power Electronics Specialist Conference*, vol. 2, June 1995, pp. 1215–1221 vol.2.

[14] J. A. Starzyk, Ying-Wei Jan, and Fengjing Qiu, "A dc-dc charge pump design based on voltage doublers," *IEEE Transactions on Circuits and Systems I: Fundamental Theory and Applications*, vol. 48, no. 3, pp. 350–359, March 2001.

[15] S. Webb, T. Liu, and Y. Liu, "Zero inductor voltage multilevel bus converter," in *2018 IEEE Applied Power Electronics Conference and Exposition (APEC)*, March 2018, pp. 2175–2182.

[16] Z. Ye, S. R. Sanders, and R. C. N. Pilawa-Podgurski, "Modeling and comparison of passive component volume of hybrid resonant switched-capacitor converters," in *2019 20th Workshop on Control and Modeling for Power Electronics (COMPEL)*, June 2019, pp. 1–8.

[17] Z. Ye, Y. Lei, W. C. Liu, P. S. Shenoy, and R. C. N. Pilawa-Podgurski, "Improved bootstrap methods for powering floating gate drivers of flying capacitor multilevel converters and hybrid switched-capacitor converters," *IEEE Transactions on Power Electronics*, pp. 1–1, 2019.

[18] EPC Inc., *Building the Smallest and Most Efficient 48 V to 5 - 12 V DC to DC Converter using EPC2045 and ICs*, 2018. [Online]. Available: https://epc-co.com/epc/Portals/0/epc/documents/application-notes/How2AppNote001\%2048\%20V\%20to\%205-12\%20V.pdf